[redacted]

Coordinated Science Laboratory

UNIVERSITY OF ILLINOIS – URBANA, ILLINOIS

CALCULATIONS CONCERNING ELECTRICAL BREAKDOWN INDUCED BY THE MELTING OF MICROSCOPIC PROJECTIONS

Donald A. Lee

REPORT R-280 January , 1966

This work was supported in part by the Joint Services Electronics Program (U. S. Army, U. S. Navy, and U. S. Air Force) under Contract Number DA 28 043 AMC 00073(E).

This work was also supported by the National Aeronautics and Space Administration under NASA Research Grant NGR-14-005-038.

Introduction

During the last several years, the understanding of the phenomenon of electrical breakdown in vacuum has been greatly advanced. It is now generally recognized that electrical breakdown between electrodes in a clean environment is initiated by field emission currents drawn from submicroscopic projections on the cathode surface,[1] the electric field at these projections being greatly enhanced from that of the average electric field which would exist in the absence of such projections. Although field emission processes were recognized early as possible mechanisms for the initiation of electrical breakdown,[2] quantitative identification was not firmly established until the investigations of Dyke,[3] and then only for the particular case of the point-to-plane geometry of the Müller[4] field emission microscope. For this geometry Dyke and his co-workers clearly demonstrated that electrical breakdown was initiated by field emission currents when the current density from the point tungsten cathode exceeded a critical value of 10^8 a/cm^2. The electric field strengths necessary to draw these current densities are of the order of $5\text{-}7\times10^7$ v/cm.[5]

Despite their definitive quality, Dyke's results did not seem consistent with results obtained with other electrode geometries. In particular, for broad area parallel electrodes the experimentally obtained electric field strengths were of the order of 10^5 v/cm,[1] two orders of magnitude lower than those found by Dyke. In addition, the electric field strengths at breakdown depended on gap spacing,[6] a fact at variance to any conceived mechanism involving field emission. With

these apparent discrepancies to a field emission theory of breakdown a plethora of other theories were advanced both before and after Dyke's startling results.[1]

Reporting in 1962, Alpert and Lee[7] analyzed the experimental results of Boyle, Kisliuk and Germer,[8] who used crossed tungsten wires at short gap spacings, and the results of Dyke and showed a previously unrecognized agreement between these two investigations: electrical breakdown occurred when the electrical field measured at the field emission sites exceeded the critical value of 6.5×10^7 v/cm to within a small experimental error. These findings were greatly extended with the experimental work of Alpert, Lee, Lyman and Tomaschke.[1] Using broad area electrodes they verified the critical field criterion for gap spacings up to 6 mm and voltages up to 250 kv. A similar analysis when applied to the results of Pivovar and Gordienko[9] and Ahern[2] and Chambers[10] showed substantial agreement for a constant field criterion for electrical breakdown.

An essential feature of this breakdown criterion is the existence of submicroscopic projections on the surface of the cathode. It has long been recognized that such projections can provide field enhancements of up to several thousand times the field in the absence of the projections.[11] Indirect experimental evidence for the existence of such points was provided by Boyle, Kisliuk and Germer.[8] They observed that the field enhancements necessary to bring their field emission current results into agreement with the Fowler-Nordheim theory were gap dependent. At small gaps approaching a few wave lengths of

light they observed that the field enhancement approached one. From this gap dependence they inferred the existence of points rather than the alternative explanation of exceedingly low work functions.[12] Tomaschke,[13] using an electron microscope and suitable small but nevertheless broad area tungsten electrodes was able to directly observe the existence of projections on the electrode surface, identify the prebreakdown emission as field emission, and establish that the critical field criterion was applicable. Independently, Little and Whitney[14] for a variety of materials observed in situ that the prebreakdown emission occurred from submicroscopic projections averaging two microns in length. Both experimenters verified that every electrical breakdown resulted in the removal of one or more emission sites.

Subsequently other investigators identified the existence of projections on the surface of the cathode. In particular, Brodie and Weissman[15] using a cylindrical field emission microscope were able to infer the existence of projections by an analysis of the shapes of the field emission patterns. Pivovar and Gordienko[9] by direct observation, apparently with an electron microscope, were able to demonstrate the existence of projections roughly two microns long on the molybdenum cathodes of their electrodes. The number of projections on broad area electrodes has been observed to be of the order of 50 to 100 per square centimeter by the aforementioned investigators and by Singer and Doolittle[16] using pin-hole x-ray camera equipment.

At present the circumstances of production of projections on the surface of the electrodes has not been fully investigated.

However, certain processes which result in the production of projections have been isolated. Without question the machining and handling of the electrodes before insertion into the vacuum system accounts for many projections. Additionally, Tomaschke[13] has noted several methods for producing projections prior to and during electrical breakdown. Brodie[17] has witnessed apparent whisker growth by the deposition of impurity materials from an auxiliary thermionic emitter. Pivovar and Gordienko[9] have noted a particularly unusual case of the production of whiskers in an electrical breakdown experiment. During the process of thoroughly outgassing their molybdenum electrodes at 2000°C, they subsequently found that a profusion of very sharp projections had been formed. An analysis of their data indicates that these whiskers enhanced the electric field by as much as 100 to 4000 times. It seems reasonable that these whiskers grew in the interval immediately after outgassing when the thermal stresses were large, and the substrate warm.

Thus the constant field criterion for electrical breakdown is firmly established. It seems apparent that electrical breakdown for clean tungsten electrodes in an ultrahigh vacuum environment is a field-emission-initiated phenomenon where the emission occurs from submicroscopic projections on the surface of the cathode. At breakdown the locally enhanced field at these projections is a constant to within experimental error as determined from the breakdown voltage and an analysis of the prebreakdown voltage-current relationship. This critical value of electric field is 6.5×10^7 v/cm for tungsten independent of the total voltage between the electrodes or of the macrogeometry of

the electrode surfaces. The results of four independent investigators are summarized in Figure 1. These results demonstrate that when properly analyzed electrical breakdown occurs at constant electric field for the nearly five orders of magnitude of electrode spacing investigated.

Transition Mechanism: Cathodic or Anodic?

The criterion that breakdown will ensue whenever the electric field at the surface of a cathode projection exceeds a critical value seems of technological interest rather than a fundamental result in the sense that it does not directly identify the initiatory event at which the transition to breakdown current occurs. It was recognized that this criterion could not of itself be used to exclude the anode from playing a role in the initiatory event.[7] However, the agreement in the experimental results summarized in Figure 1 is in itself a persuasive argument that the cathode is the initiatory surface. These results clearly indicate that the breakdown field is independent of all geometrical considerations. Geometries in which the role of the anode is clearly excluded, as in the point-to-plane investigations of Dyke,[3] have the same breakdown field as the broad-area, short-gap electrode investigations in which the role of the anode cannot be obviously dismissed. From these considerations alone it seems plausible to assume that the cathode surface is indeed the initiatory surface.

There is additional indirect evidence which supports the contention that the cathode surface is the initiatory surface. Tomaschke,[13] and independently Little and Whitney,[14] as well as

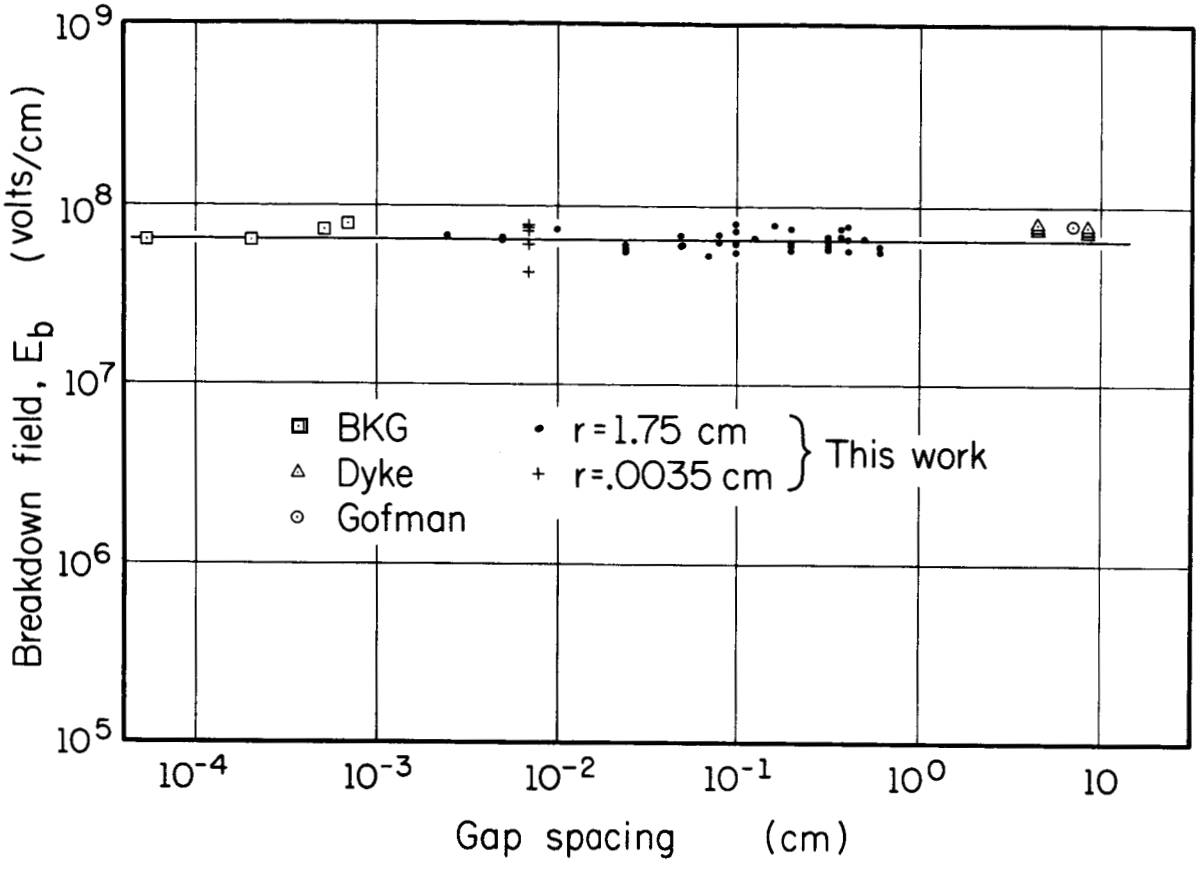

Figure 1. Summary of the Results of Four Independent Investigators for Local Electric Field at Breakdown.

Brodie,[17] find that, coincident with electrical breakdown, one or more emission sites is always destroyed. The conclusion that the cathode surface is the initiatory surface is also consistent with the experimental findings of Pivovar and Gordienko.[9] In their experiments they found that imposing a transverse magnetic field sufficiently strong to prevent the field emission current from striking the anode surface did not materially improve the voltage-holding capabilities of the electrodes. Finally, in a recent paper by Brodie,[17] it is shown that for nickel the cathode marks which result from the breakdown process are nearly identical, independent of electrode geometry. The cathode marks found on a nickel wire cathode of a cylindrical field emission microscope were indistinguishable from the cathode marks found on a nickel broad area cathode.

But even for larger gap spacings up to 6 mm, where field emission techniques have been used for broad area electrodes, the experimental results tend to support a field emission mechanism. For such gaps, it is found that the voltage-holding capability increases and the background current decreases when a gas is introduced[18] into the gap spacing at a pressure of the order of 10^{-4} Torr. The only plausible explanation thus far presented for this effect is associated with the selective destruction of cathode projections by ion bombardment. Similarly, the experimental results of Murray[19] using hot glass cathodes and Rohrbach[20] and Jeydnck[21] using coated cathodes (coated with high dielectrics to reduce the cathode fields) to obtain higher breakdown voltages are consistent with a cathode-initiating event.

We are not aware of experimental results which support the contention that the anode is involved in the breakdown transition to high currents. No process has been postulated which can generate ions in sufficient numbers to directly increase the interelectrode current by the orders of magnitude necessary in the transition.[22] For some experiments, transition time consideration would seem to prevent the anode from even augmenting the field emission current through any known space charge mechanism.[23] Particularly the calculations of Kisliuk[24] indicate that the increase in field emission current due to the close approach of single ions to the cathode surface is especially small for large gaps. Mechanisms involving the vaporization of the anode material[25] by field emission currents followed by gas breakdown in the vapor do not seem plausible. Experiments in electron beam welding[26] indicate that electron beams may have penetration depths orders of magnitude longer than those predicted by Waddington's law[27] for single electrons. These experimental results bring into serious question the validity of the calculations of the amount of gas vapor evaporated from the anode. Additionally, no secondary effects of this gas cloud, such as the condensation of the vapor on other surfaces, have been noted in the literature.

In summary, there seems to be strong evidence that the cathode is the initiatory surface, and conversely, little evidence that would demand or even allow the anode to take part in the transition to breakdown.

A Review of Cathode Transition Mechanisms

From their results in the point-to-plane geometry, Dolan, Dyke and Trolan[28] calculated that the field emission current densities just prior to breakdown were sufficient to melt the cathode projection. Dyke,[3] et al., proposed a regeneration scheme whereby the cathode current is greatly increased through the creation of positive ions by electron impact processes in the metallic vapor evaporated at these elevated temperatures. It does not seem reasonable that this process could be a general process applying to all materials. Not only is there no discontinuity in the vapor pressure at the melting point, but there are orders of magnitude difference in the vapor pressures of common materials at their melting points.[29] Furthermore, the experiments of Gorkov[30] in which the field emission processes were investigated at high pressures, of the order of 10^{-4} Torr, gave no evidence that the negative space charge found in field emission microscope experiments could be neutralized.

Vibrans[31] has analyzed the temperature-field emission process itself and has shown it to be unstable. He points out that the field emission current increases the temperature at the surface of the projection through ohmic heating, and this increase in the temperature increases the current through thermal emission processes. The process so envisioned is unstable, leading to a rapid buildup of the current. However, Vibrans did not take into consideration cooling from the Nottingham effect[32] which will tend to stabilize the temperature of the surface to a value dependent solely on the field. Experiment also

argues against the phenomenon since field emission has been shown to be stable and reproducible up to the point of breakdown. At these high fields the current does not depend strongly on temperature. However, there may be cases in which the Vibrans model can be shown to dominate over the cooling effects of the Nottingham process. An example is the case of long whiskers in which sufficient ohmic heating can occur at low fields to overcome the Nottingham effect.

A Suggested Transition Mechanism

An alternative mechanism for the initiatory event has been suggested by Alpert, Lee, Lyman and Tomaschke[1] in which the field emission currents heat the projection up to a temperature, perhaps the melting temperature, where the mechanical strength of the projection fails. They postulate that the projection then becomes strongly unstable and the electrode material begins to move into the gap under the action of the strong electrical forces. This process could either greatly enhance the electric field at the surface or increase the emitting area, or both, resulting in a large increase in the field currents. It is suggested that this process can lead to a situation closely paralleling the exploding wire experiments of Tucker.[33] In these experiments current densities comparable to those obtained in field emission experiments melt and vaporize the wire in a nanosecond's time. If in an analogous manner the projection melts and vaporizes, then it is seen that conditions are established that are ideally suited for the transition to a low-voltage, high-current arc.

This mechanism is consistent with the experimental breakdown results obtained from field emission microscope studies with tungsten cathodes. Mechanical failure at the melting point is a reasonable assumption for tungsten, since breakdown fields for tungsten are substantially less than the field strengths of 6×10^8 v/cm necessary for the rupture of the point anodes of field-ion microscopes.[34]

The Calculation of the Critical Field for Tungsten

It remains to reconcile the experimental fact that breakdown occurs at a more or less constant electrical field with the proposed melting mechanism for electrical breakdown. At first glance, it would seem to follow that if breakdown occurs at constant field then all of the projections on the cathode surface should look more or less alike; a conclusion directly refuted by our experiments. To investigate this seemingly contradictory conclusion we have analyzed this proposed mechanism for electrical breakdown by conducting a computer analysis to determine the field necessary to bring idealized projection shapes to a critical temperature. It is shown that for a vast variety of emitter sizes and shapes, roughly corresponding to those experimentally observed, electrical breakdown will occur by the proposed mechanism for electric fields in a range within the experimental error associated with the experiments summarized in Figure 1.

In the course of carrying out these calculations, several more accurate approximations for the field-temperature dependent electron emission were found in the literature. Numerical calculations

based on these new approximations have not previously been made. Supplementary calculations representing small corrections to field-temperature emission and the Nottingham critical temperature are also given.

It is recognized that the melting of the projection is principally due to the field emission currents. Before we calculate the critical field necessary to melt the projections, we will briefly review both the field emission theory and the Nottingham effect.

A. Combined Temperature and Field Dependent Emission.

Field emission was recognized by Fowler and Nordheim[35] as a quantum mechanical problem in which the electrons of the conduction band are pictured as tunnelling through the field reduced potential barrier of the metal as can be seen in Figure 2. Fowler and Nordheim, using the energy distribution of the electrons within the conduction band as a function of temperature found by Sommerfield, calculated the rate of arrival of electrons at the boundary. Upon calculating the transparency of the boundary as a function of energy, they found that by taking the low temperature limit they could obtain in closed form the field-dependent current density. Fowler and Nordheim combined as a final result the following expression for the dependence of current density J on electric field:[36]

$$J = [1.54\times10^{-6}E^2/\varphi t^2(y)] \cdot \exp -6.83\times10^7(\varphi^{3/2}/E(y)) \qquad (1)$$

where E is the electric field at the cathode surface, φ is the work function of the cathode material, and v and t are slowly varying

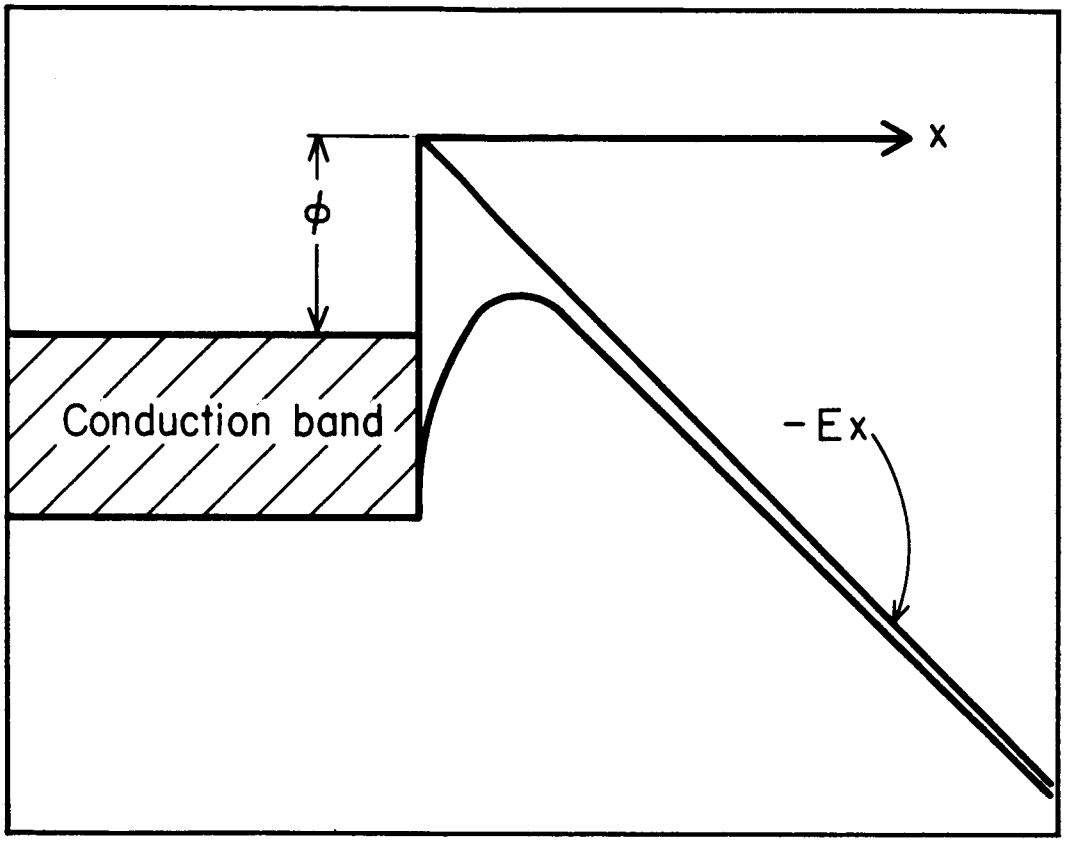

Figure 2. Schematic Diagram of Field Emission. The conduction electrons are pictured as tunneling through the field-reduced potential barrier.

functions of the variable $y = (s \cdot 79 \times 10^{-4} E^{\frac{1}{2}})/\varphi$, which are almost constant over the useful range of measurements of the current density.

Temperature corrections to field emission have been made by Dyke,[37] Brodie,[38] and Gorkov, Elinson and Yakovleva.[39] However, the validity of these corrections is in some question at temperatures and fields where significant electron populations exist at energy levels near and above the height of the field reduced potential barrier. At these energy levels their approximations for the transparency of the barrier give unity probability for emission which in essence treats the electron as a classical particle.

Murphy and Good,[40] using a more general form for the transparency of the barrier as a function of electron energy, found by Kemble,[41] have derived expressions for the combined temperature-field emission more accurate at all temperatures and fields. In particular, Murphy and Good have shown that their expressions give as limiting cases field emission and thermal emission.

It is not the intention herein to give complete derivations of the particular results since the reader for himself may consult the references for this, but rather to give those results necessary to calculate the combined temperature-field emission. The energy distribution of the electrons in the metal is such that N(w) electrons per second in the energy range dw arrive at the boundary of the metal. Fowler and Nordheim formulate N(w) as follows:

$$N(w) = \frac{4\pi mkT}{h^3} \log\left(1 + \exp - \frac{w+\varphi}{kT}\right)$$

where m is the mass of the electron,
k is the Boltzmann constant,
T is the temperature in ^{o}K,
h is Planck's constant,
φ is the work function.

Now the probability D(w) that an electron penetrates the field-reduced barrier a and escapes as formulated by Murphy and Good is:

$$D(w) = \frac{1}{1+\exp \frac{4\sqrt{2mw^3}}{3\hbar eF} v(y)}$$

where $\hbar$ is $h/w\pi$,
F is the electric field,
v(y) is a function of the complete Elliptic Integrals.

$$y = \sqrt{e^3F}/|w|$$

for $0 < y < 1.0$.

$$v(y) = (1+y)^{\frac{1}{2}}E[(1-y)^{\frac{1}{2}}/(1+y)^{\frac{1}{2}}] - yK[(1-y)^{\frac{1}{2}}/(1+y)^{\frac{1}{2}}]$$

for $y > 1.0$.

$$v(y) = -(y/2)^{\frac{1}{2}} - 2E[(y-1)^{\frac{1}{2}}/(2y)^{\frac{1}{2}}] + (y+1)K[(y-1)^{\frac{1}{2}}/(2y)^{\frac{1}{2}}]$$

where K(k) and E(k) are the complete Elliptic Integrals of the first and second kind, respectively.

The current density for a particular temperature and field is found by numerically integrating the product of N(w) and D(w) over the energy range within the metal:

$$j = e \int_{-\infty}^{o} D(w)N(w)dw$$

where

j is the current density,
e is the electronic charge,
w is the energy of the incident electron,
D(w) is the transmission coefficient,
N(w) is the flux of electrons incident to the surface.

The results of the calculations are given in Figure 3, where the common logarithm of the current density is given as a function of both the electric field and the temperature.

B. The Nottingham Effect

One of the fundamental assumptions of the field emission calculation is that the electron distribution within the metal is the steady-state distribution found by using Fermi-Dirac statistics. This is a reasonable assumption since even at the highest current densities found experimentally only a small percentage of the electrons in the metal which strike the barrier also penetrate it. Nottingham[32] recognized that when the emitted electrons are replaced in the distribution within the metal an energy exchange process develops between the crystal lattice and the electron distribution. Postulating that this electron must come from the Fermi level, Nottingham predicted that the emission current may either heat or cool the surface depending on whether the majority of the emitted electrons

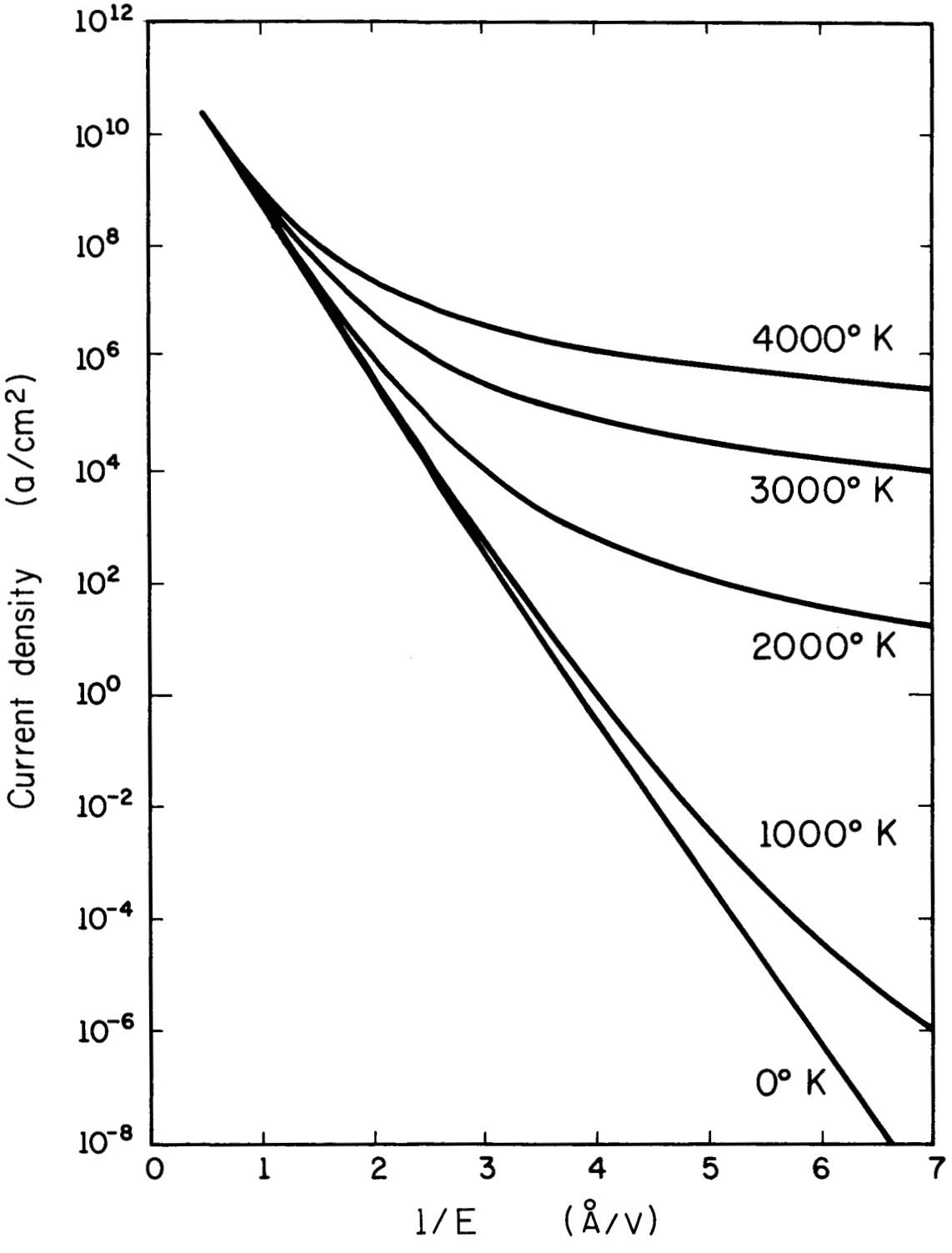

Figure 3. Field Emission Current Density as a Function of Field and Temperature.

come from below the Fermi level or from above it. Thus if the emitted electron comes from below the Fermi level, the electron from the Fermi level used to fill this vacancy gives up energy to the lattice leading to Nottingham heating. Alternatively when the electron is emitted from above the Fermi level, the lattice must supply the energy necessary to excite an electron from the Fermi level to replace the emitted electron, thus leading to Nottingham cooling of the surface.

These effects can clearly be seen in the interpretation of the normalized current densities in Figures 4 and 5. Here the emitted electron energy distributions are plotted. They are obtained by evaluating at a given temperature and field the product of the transparency of the barrier D(w) and the rate of arrival N(w) used in the last section to determine the current density. Although the actual current densities differ by orders of magnitude it is only the symmetry with respect to the Fermi level which will determine whether the Nottingham effect will be heating or cooling. The magnitude of the effect nevertheless will depend on the magnitude of the current density.

Consider Figure 4 in which three different electron distributions for the same temperature but differing fields are shown. It will be seen that as the field is increased the number of electrons penetrating the barrier below the Fermi level is increased. Alternatively, as can be seen in Figure 5, increasing the temperature increases the number of electrons in the energy levels above the Fermi level, thus shifting the distribution toward higher energy levels.

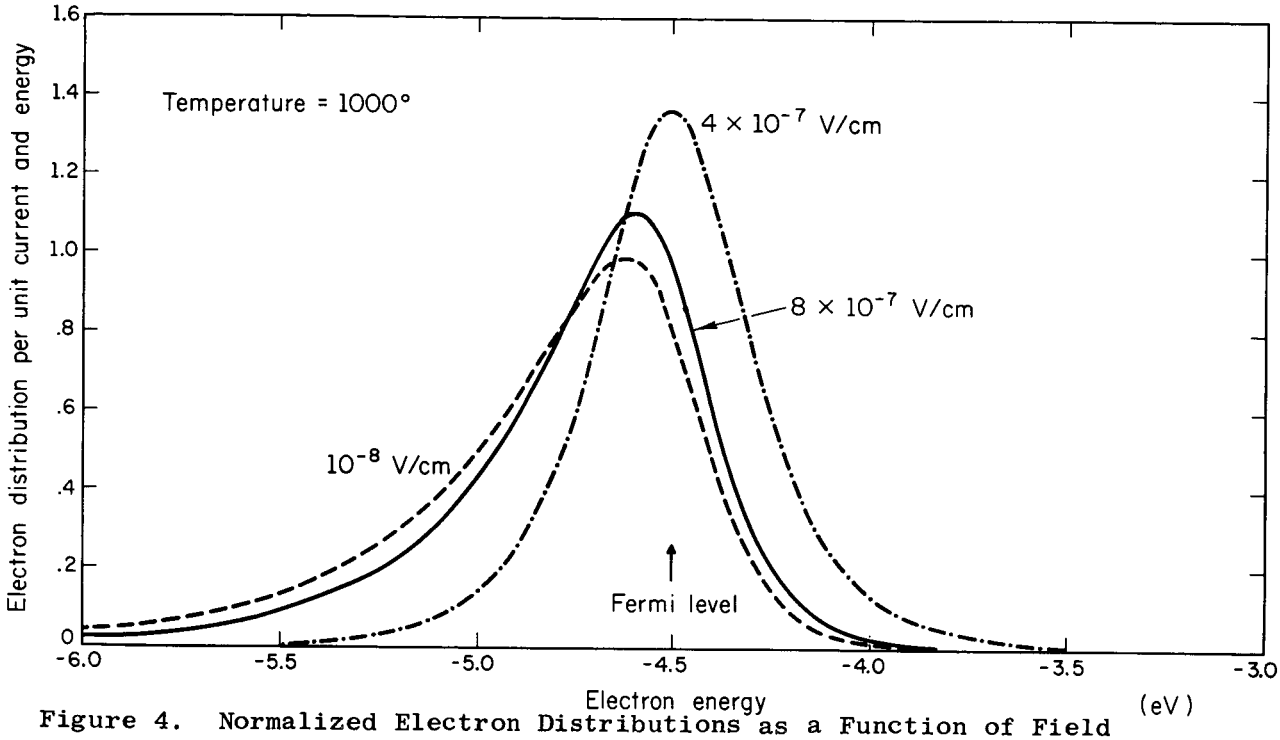

Figure 4. Normalized Electron Distributions as a Function of Field at Constant Temperature. The curves are normalized to equal areas.

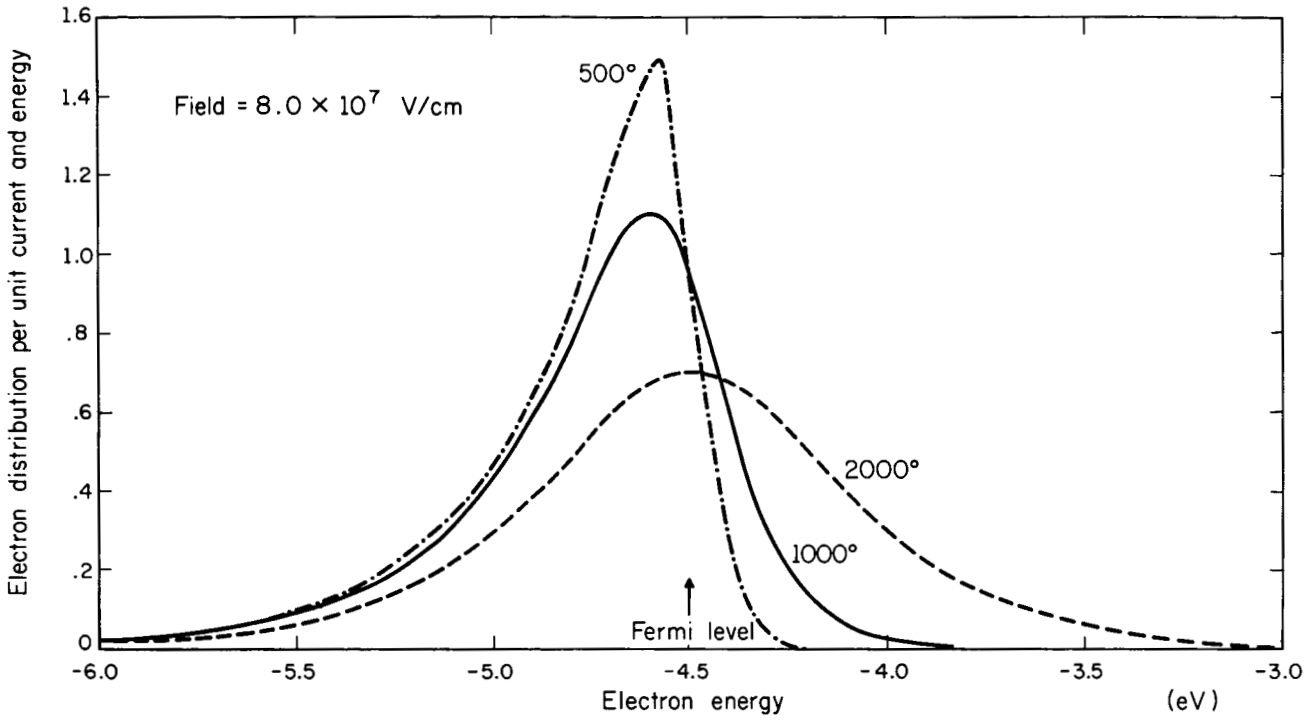

Figure 5. Normalized Electron Distributions as a Function of Temperature at Constant Field.

It was recognized by I. Brodie[38] that if the other sources of heating and cooling could be ignored, the Nottingham effect would stabilize the temperature of the emitting surface to a temperature which was solely dependent on the electric field. At this temperature, called the critical temperature by Levine,[42] the energy which the lattice supplied for the electrons emitted above the Fermi level is exactly equal to the energy received by the lattice for electrons emitted below the Fermi level. Thus if the temperature of the surface is below the critical temperature more electrons are emitted below the Fermi level than above, giving rise to Nottingham heating, which will tend to bring the temperature of the surface to the critical temperature. Increasing the electric field increases the number of electrons emitted below the Fermi level thus demanding that the inversion temperature increase.

The Nottingham effect can be formulated as follows:

$$NT = e \int_{-\infty}^{o} \int_{-\infty}^{E} (w+\varphi) D(w) N(E,w) dE dw$$

where the functions D(w) and N(w) have the same significance as in the current density calculation. However, account must be taken of the fact that the original electron distributions found by Fowler and Nordheim were distributions of normal energy of the electron with respect to the barrier. Young[43] has considered this and has reformulated the supply function as a function of both total energy and of the normal energy component of the total energy as:

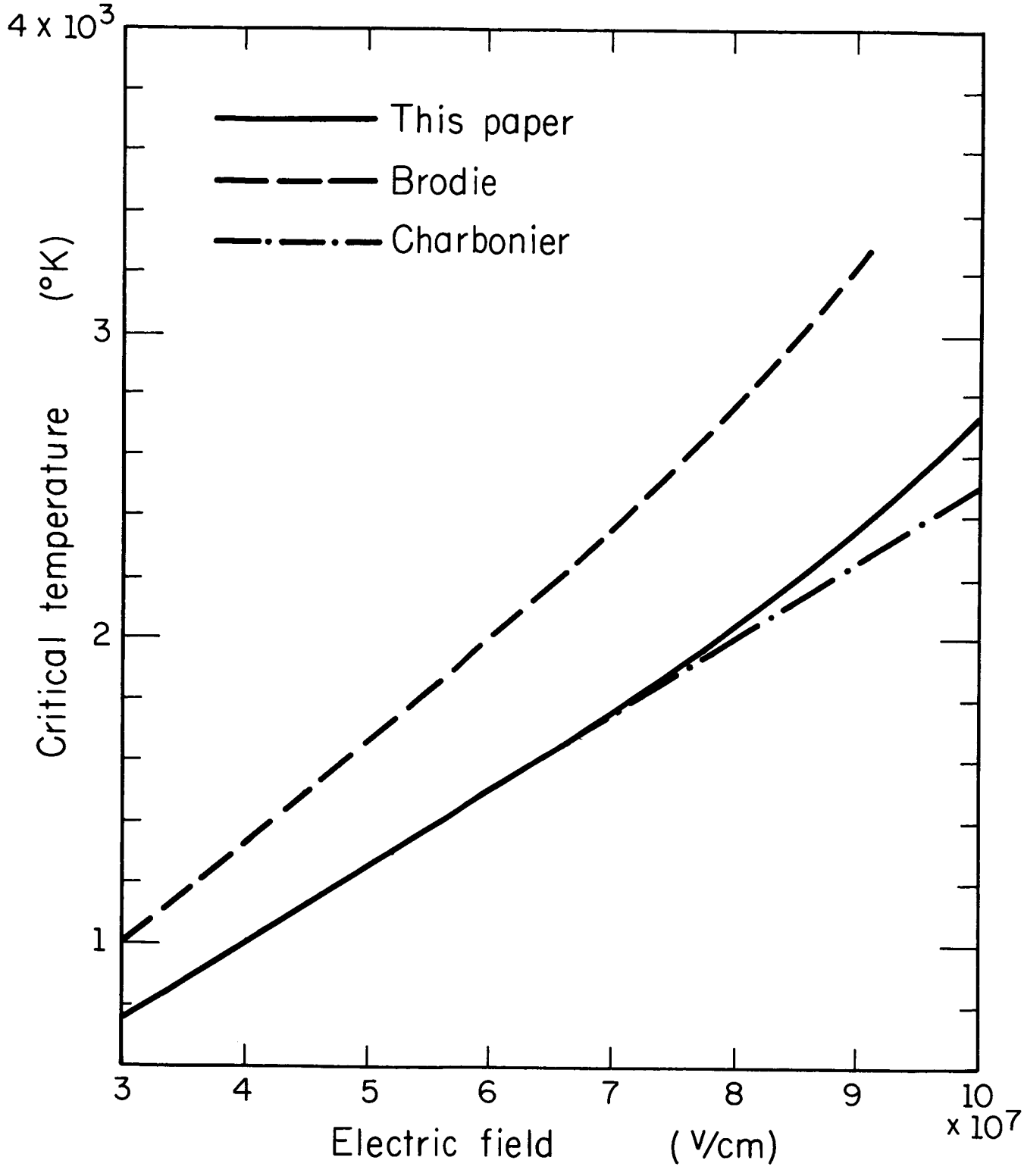

Figure 6. The Critical Temperature as a Function of the Field.

temperature distribution must be fitted. The assumption that the Nottingham effect is solely a surface effect demands that the transfer of energy to and from the metal lattice occur very near the surface. There is no experimental justification for this assumption. Indeed the energy transfer may occur deep within the metal by a multiple step transition process. If this were the situation then the effects of the Nottingham process on the temperature of the surface and on the temperature distribution in the projection would be greatly exaggerated. However, in the absence of direct experimental evidence in regard to this point we make the assumption that the process occurs at the surface allowing us to include the Nottingham effect as a boundary condition rather than as a more mathematically cumbersome volume heating or cooling effect.

It should be noted that calculation of the critical temperature is not dependent on where the energy transfer takes place but is only a function of the field at the surface and the electron. The steady state heat conduction equation:[44]

$$K\nabla^2 T = -g(x,y,z)$$

where $g(x,y,z)$ is the source function.

For radial symmetry in a spherical coordinate system and for the case of resistive heating the conduction equation reduces to a second order differential equation as follows:

$$\frac{1}{r^2}\frac{d}{dr}\left(r^2\frac{dT}{dr}\right) = -\frac{\rho}{K}j^2(r)$$

where ρ is the resistivity of the medium and K, the thermal conductivity. If we let j_o be the field emission current density at the emission surface and r_o the location of the emission surface then the differential equation assumes the final form:

$$\frac{1}{r^2}\frac{d}{dr}\left(r^2\frac{dT}{dr}\right) = -\frac{\rho}{K} j_o^2 \left(\frac{r_o}{r}\right)^4 .$$

It should be noted that the equation may be solved analytically for the case in which the resistivity and the thermal conduction are not functions of the temperature. However, in the range of interest here the resistivity varies by a factor of nearly twenty and the equation must be solved by numerical means.

The numerical solution is found by stipulating the temperature and the field at the emission site. The field and the temperature are sufficient to specify the Nottingham effect, and it is used to determine the initial value of the dT/dr since KdT/dr is the energy transported across the emission site by the Nottingham effect. Thus the field and the temperature at the emission site are used for adjustable parameters in the calculation to find appropriate solutions which have as a maximum temperature the melting point of tungsten and room temperature at the cold end of the projection.

Numerical Methods

The numerical integration of the heat equation as well as the temperature-field emission and the Nottingham effects was accomplished using the methods developed by A. Nordsieck.[45] In this

method the integration step size is controlled by the integration routine to assure convergence to a solution as well as to control the integrated error.

The error sizes were chosen so as to assure at least four significant figures. In this calculation, the resistivity and the heat conduction were both considered functions of the temperature. The approximations used were found by the methods presented by Hastings.[46] In particular, the experimental data of Langmuir[47] were fitted to a third order polynomial to achieve a nearly Chebyshev error of $\pm$ .2 ohms/cm over the range from 300°C to the melting temperature of tungsten. Experimental values of the thermal conductivity are not available over this entire range. Thus recourse had to be made to the Wiedemann-Franz Ratio[48] to approximate the thermal conductivity. A ratio of two third-order polynomials was chosen to fit the available data of Langmuir[49] and Holliday and Worthington.[50] The high temperature values were determined by the requirement that the high temperature limit ratio approach the theoretical value[48] of

$$\frac{\pi^2}{3}\frac{k^2}{2} = 2.45 \times 10^{-8} .$$

The errors in the approximation for the coefficient of heat conduction when compared to the experimental values were random in nature. The formulations for the resistivity, ρ, and thermal conductivity, K, used in the calculations are:

$$10^6\rho = -1.8851+23.6572T/(10^3)+3.2696T^2/(10^6)-.2325T^3/(10^9) \ .$$

$$K(T) = \frac{TL(T)}{\rho}$$

where L(T) =

$$\frac{3.92108-2.16520T/(10^3)-1.79225T^2/(10^6)+2.45T^3/(10^9)}{1.17466-.18169T/(10^3) = 1.15563T^2/(10^6)+T^3/(10^9)} \times 10 \ .$$

Finally, the complete elliptical integrals were evaluated using Hastings'[46] formulation which gives about six decimal places of accuracy.

Results of the Calculation

The results of the calculations of the temperature distributions are summarized in Figures 7 and 8. In Figure 7 is shown the critical field as a function of the length and cone angle. The critical field is the field for which some portion of the projection will be near the melting point. Notice that the actual length of the whisker does not become important until the cone angle becomes very small. For conical projections the important parameter is the emitting area.

In Figure 8 we present the temperature distributions along one micron length projections of various cone angles. Notice that at small cone angles the distribution is approximately parabolic as is the case for cylindrical projections. However, as the cone angle is increased, the distribution becomes a nearly $1/r^2$ law.

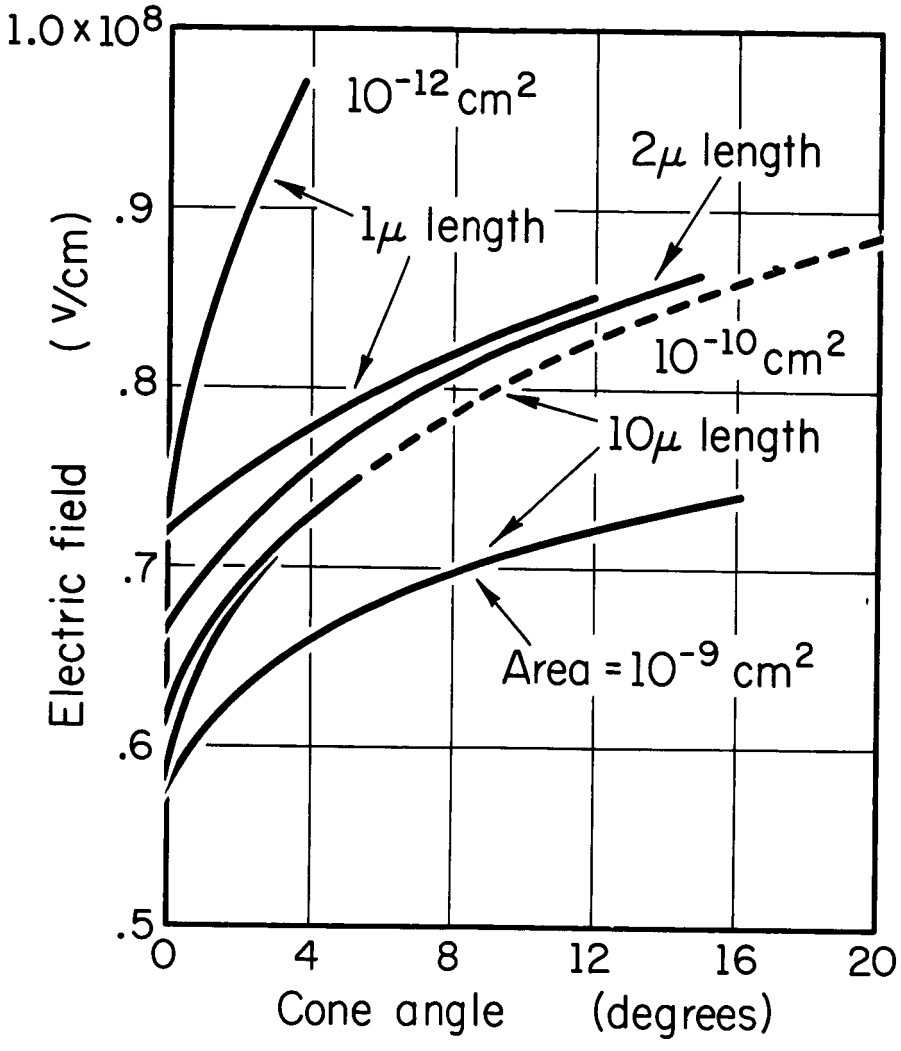

Figure 7. The Critical Field as a Function of the Length and Cone Angle.

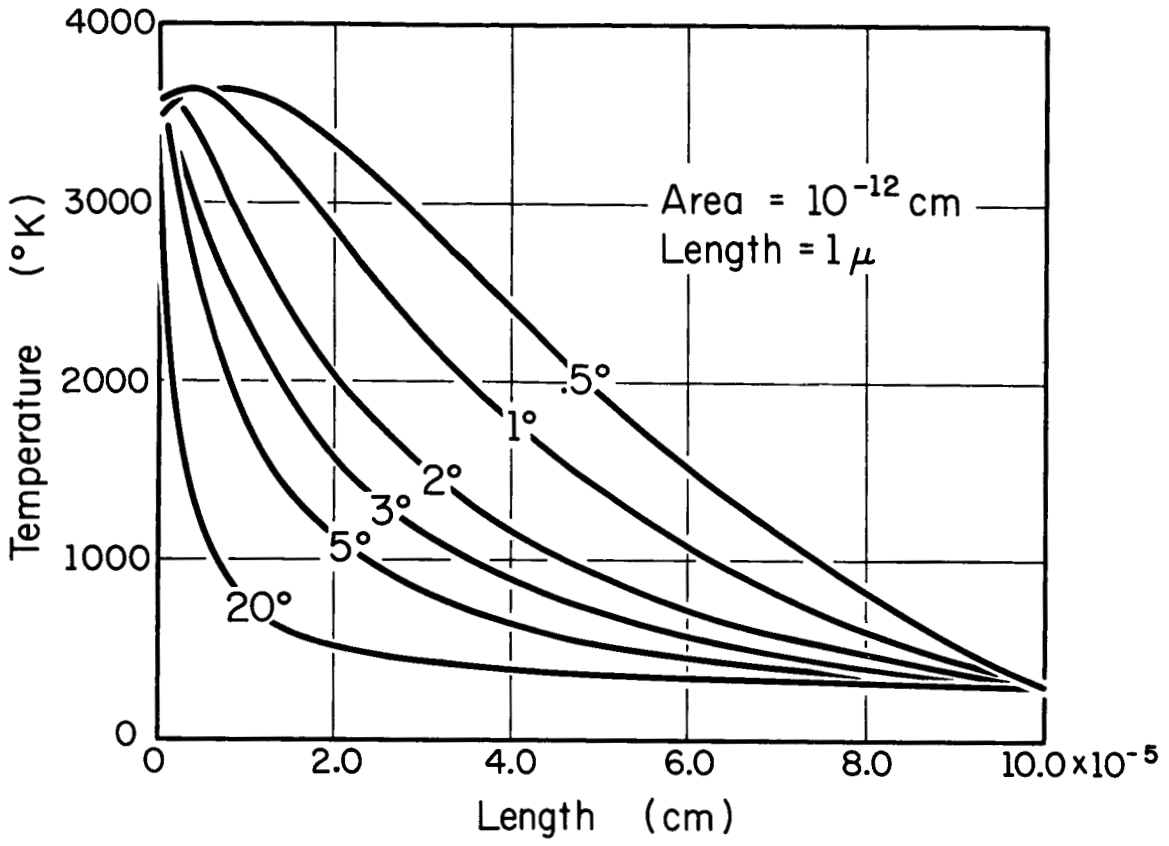

Figure 8. Temperature Distribution along One Micron Length Projections as a Function of Various Cone Angles. All the cases are situations in which the maximum temperature is equal to the melting temperature.

It is interesting to note that the average breakdown field gives a critical length for a cylinder of roughly 2 microns, a length which is consistent with our experimental findings and with those of Little and Whitney.[14] From the conical results we note that if breakdown proceeds via the proposed mechanism, it must be associated with projections of small cone angle.

Concluding Discussion

The results of the calculations clearly indicate the plausibility of the theory that breakdown occurs at or near the field necessary to bring the temperature of the projection to the melting point of tungsten. The curves also indicate the reason for describing electrical breakdown as a field phenomenon. Since the experimental error of the observations, $\pm 1 \times 10^7$ v/cm, encompasses nearly two orders of magnitude of critical length in the cylindrical case, then minor variations in emitter geometry would require only insignificant changes in the field to achieve breakdown.

This fantastic variation of the critical length with electric field is a direct consequence of the equally fantastic variation of current with field. In Figure 9 we plot current density versus electric field for three different work functions. It can be seen that for all substances, an increase of field at one order of magnitude from 10^7 to 10^8 volts/cm gives rise to as much as 20 orders of magnitude increase in current density. It is therefore not surprising

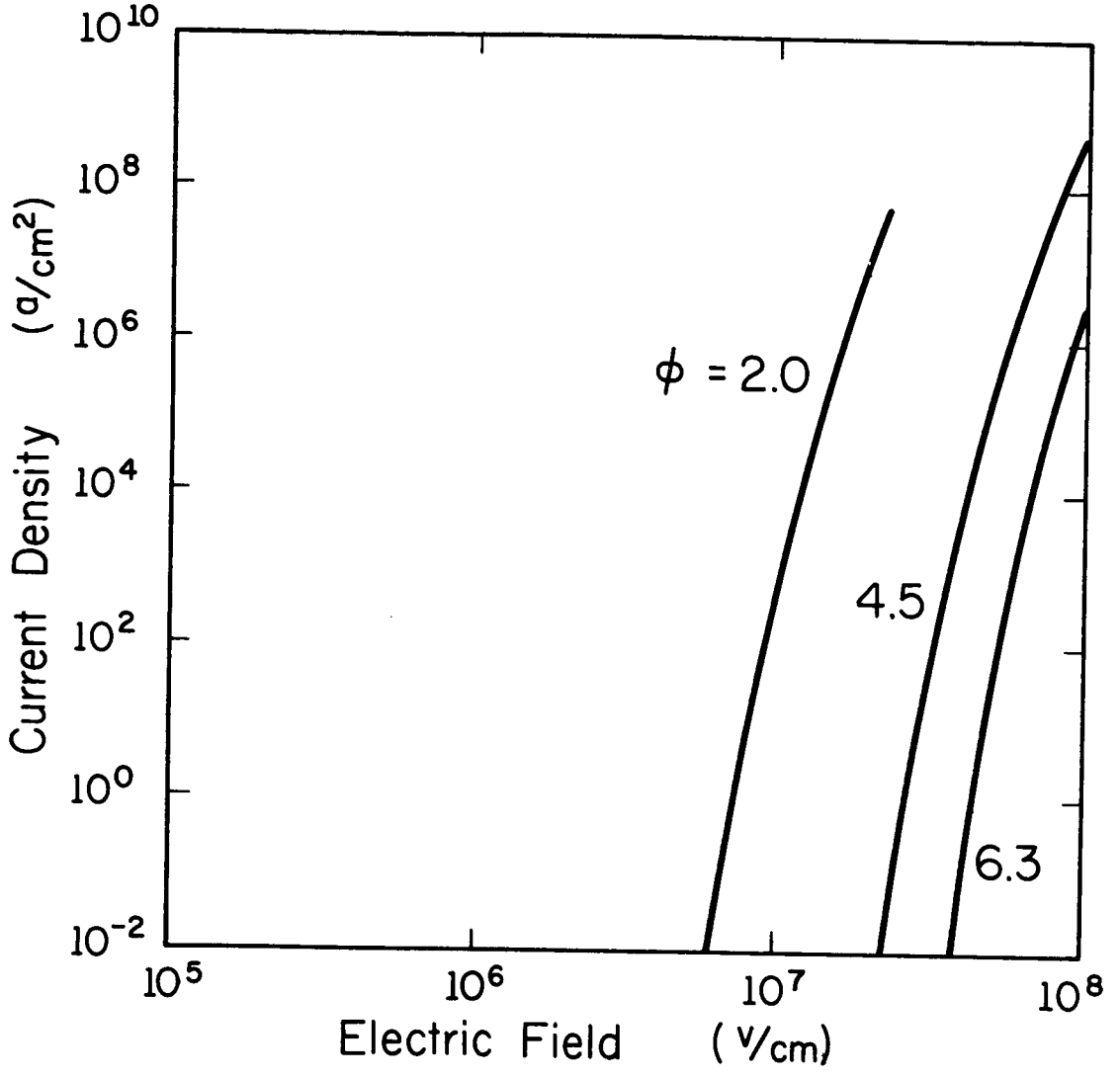

Figure 9. Fowler-Nordheim Current Density as a Function of Electric Field. Notice that one order of magnitude change in electric field produces more than fourteen orders of magnitude change in current density.

to expect something violent to occur when one runs into this brick wall of field emission.

We suggest that electrical breakdown in vacuum is a process in which a projection on the cathode surface is heated until the electrode becomes mechanically unstable and the weakened material is drawn into the electrode gap under the influence of the strong electric fields. In this circumstance the field emission current will be further enhanced since the field will be rapidly increasing due to the changing geometry. The enhanced current then allows for more heating of the material leading to further current buildup. The field emission process then presents a self-consistent picture of electrical breakdown in which no recourse is made to the use of adjustable parameters to fit experiment to theory.

REFERENCES

1. D. Alpert et al., Journ. Vac. Sci. & Techn. 1, 35 (1964).

2. A. J. Ahearn, Phys. Rev. 50, 238 (1936).

3. W. P. Dyke and J. K. Trolan, Phys. Rev. 89, 799 (1953); W. P. Dyke, J. K. Trolan, E. E. Martin, and J. P. Barbour, Phys. Rev. 91, 1043 (1953); and W. W. Dolan, W. P. Dyke, and J. K. Trolan, Phys. Rev. 91, 1054 (1953).

4. E. W. Müller, Z. Physik 106, 541 (1937); 668 (1938).

5. For a detailed presentation of the theory of field emission, see R. H. Good, Jr., and E. W. Müller, Handbuch der Physik (Springer-Verlag, Berlin, 1956), vol. 21, p. 176.

6. H. W. Anderson, Elec. Eng. 54, 1315 (1935).

7. D. Alpert and D. Lee, CSL Report R-129 (June, 1962).

8. W. S. Boyle, P. Kisliuk, and L. H. Germer, J. Appl. Phys. 26, 720 (1955).

9. L. I. Pivovar and V. I. Gordienko, Sov. Phys.-Tech. Phys. 7, 908 (1963).

10. C. C. Chambers, J. Franklin Inst. 218, 463 (1934).

11. This technique was first used by R. Haefer, Z. Physik 116 (1940); W. Schottky, Z. Physik 14, 63 (1923); and T. J. Lewis, J. Appl. Phys. 26, 1405 (1955).

12. F. Llewellyn Jones, Proceedings of the Royal Society A119, 173 (1928).

13. H. Tomaschke, "Study of the Projections of Electrodes and Their Effect on Electrical Breakdown in Vacuum," Ph.D. thesis, University of Illinois (1964).

14. R. P. Little and S. T. Smith, J. Appl. Phys. 36, 1502 (1965); and R. P. Little and W. T. Whitney, J. Appl. Phys. 34, 2430 (1963).

15. J. N. Anno, Nuclear News 5, 3 (1962).

16. B. Singer and H. D. Doolittle, J. Appl. Phys. 36, 2002 (1965).

17. I. Brodie, Journ. Vac. Sci. & Techn. 2, 249 (1965).

18. E. G. Linder and S. M. Christian, J. Appl. Phys. 23, 1213 (1952).

19. J. J. Murray, Univ. Calif. Rad. Lab. Rept. 9506 (1960).

20. F. Rohrback, Proc. International Symposium on Insulation of High Voltages in Vacuum, MIT, 393 (1964); private communication.

21. L. Jedynak, Journ. Appl. Phys 35, 1727 (1964).

22. I. Langmuir, Phys. Rev. 33, 954 (1929).

23. H. Heard, Univ. Calif. Rad. Lab. Rept. AEC-UCRL-2251.

24. P. Kisliuk, J. Appl. Phys. 30, 51 (1959).

25. A. Maitland, J. Appl. Phys. 32, 2399 (1961); and W. S. Boyle, P. Kisliuk, and L. H. Germer, J. Appl. Phys. 26, 720 (1955).

26. Electron beam welds extend as deep as three inches in stainless steel with 100 keV electrons.

27. L. E. Glendenin, Nucleonics 2, 12 (1948).

28. W. W. Dolan, W. P. Dyke, and J. K. Trolan, Phys. Rev. 91, 1054 (1953).

29. S. Dushman, Scientific Foundations of Vacuum Technique (John Wiley & Sons, New York, 1962), p. 696.

30. V. A. Gor'kov, M. I. Elinson, and G. D. Yakovleva, Radio Engr. and Electronic Phys. 9, 409 (1962).

31. G. E. Vibrans, Report on the 24th Annual Conf. on Physical Electrons, MIT (1964).

32. W. Nottingham, Phys. Rev. 59, 907 (1941).

33. T. Tucker, J. Appl. Phys. 32, 1894 (1961).

34. E. Cooper and E. Müller, Rev. Sci. Instr. 29, 309 (1958).

35. R. H. Fowler and L. Nordheim, Proc. Roy. Soc. A119, 173 (1928).

36. L. Nordheim, Proc. Roy. Soc. A121, 626 (1928).

37. W. W. Dolan, W. P. Dyke, and J. K. Trolan, Phys. Rev 91, 1054 (1953).

38. I. Brodie, private communication.

39. V. A. Gor'kov, M. I. Elinson, and G. D. Yakovleva, Radio Engr. and Electronic Phys. 9, 1404 (1962).

40. E. L. Murphy and R. H. Good, Phys. Rev. 102, 1464 (1956).

41. E. C. Kemble, The Fundamental Principles of Quantum Mechanics, (Dover Publications, Inc., New York, 1959), p. 109 ff.

42. P. H. Levine, J. Appl. Phys. 37, 582 (1962).

43. R. D. Young, Phys. Rev. 113, 110 (1959).

44. W. W. Dolan, W. P. Dyke, and J. K. Trolan, Phys. Rev. 91, 1054 (1953).

45. A. Nordsieck, Mathematics of Computation 16, 22 (1962).

46. C. Hastings, Approximations for Digital Computers (Princeton University Press, Princeton, 1955), gives expansions for these functions suitable for use with a digital computer.

47. I. Langmuir, Phys. Rev. 7, 302 (1916).

48. C. Kittel, Introduction to Solid State Physics (John Wiley & Sons, New York, 1956), p. 241.

49. I. Langmuir, Phys. Rev. 7, 302 (1916).

50. A. G. Worthington and D. Halliday, Heat (John Wiley & Sons, New York, 1948), p. 496.

Security Classification

DOCUMENT CONTROL DATA R&D

(Security classification of title, body of abstract and indexing annotation must be entered when the overall report is classified)

1. ORIGINATING ACTIVITY (Corporate author)
University of Illinois
Coordinated Science Laboratory
Urbana, Illinois 61801

2a. REPORT SECURITY CLASSIFICATION
Unclassified

2b. GROUP

3. REPORT TITLE

CALCULATIONS CONCERNING ELECTRICAL BREAKDOWN INDUCED BY THE MELTING OF MICROSCOPIC PROJECTIONS

4. DESCRIPTIVE NOTES (Type of report and inclusive dates)

5. AUTHOR(S) (Last name, first name, initial)

Lee, Donald A.

6. REPORT DATE	7a TOTAL NO. OF PAGES	7b. NO. OF REFS.
January, 1966	35	50

8a. CONTRACT OR GRANT NO.
DA 28 043 AMC 00073(E)
b. PROJECT NO. 20014501B31F
Also National Aeronautics and
c. Space Administration under Grant
d. NGR-14-005-038

9a. ORIGINATOR'S REPORT NUMBER(S)
R-280

9b. OTHER REPORT NO(S) (Any other numbers that may be assigned this report)

10. AVAILABILITY/LIMITATION NOTICES
Qualified requesters may obtain copies of this report from DDC.
This report may be released to OTS.

11. SUPPLEMENTARY NOTES

12. SPONSORING MILITARY ACTIVITY
U. S. Army Electronics Command
Ft. Monmouth, New Jersey 07703

13. ABSTRACT

16187

Calculations have been made concerning electrical breakdown induced by the melting of microscopic projections on the cathode surface. A digital computer analysis of tungsten shows a surprising correlation between measured electrical breakdown fields and the fields necessary to melt tungsten projections.

(author)

DD FORM 1 JAN 64 1473

Security Classification

Security Classification

KEY WORDS	LINK A		LINK B		LINK C	
	ROLE	WT	ROLE	WT	ROLE	WT
electrical breakdown in ultrahigh vacuum field emission currents microscopic projections, melting of cathode surface cathode transition mechanisms Nottingham effect properties of tungsten						

INSTRUCTIONS

1. ORIGINATING ACTIVITY: Enter the name and address of the contractor, subcontractor, grantee, Department of Defense activity or other organization (corporate author) issuing the report.

2a. REPORT SECURITY CLASSIFICATION: Enter the overall security classification of the report. Indicate whether "Restricted Data" is included. Marking is to be in accordance with appropriate security regulations.

2b. GROUP: Automatic downgrading is specified in DoD Directive 5200.10 and Armed Forces Industrial Manual. Enter the group number. Also, when applicable, show that optional markings have been used for Group 3 and Group 4 as authorized.

3. REPORT TITLE: Enter the complete report title in all capital letters. Titles in all cases should be unclassified. If a meaningful title cannot be selected without classification, show title classification in all capitals in parenthesis immediately following the title.

4. DESCRIPTIVE NOTES: If appropriate, enter the type of report, e.g., interim, progress, summary, annual, or final. Give the inclusive dates when a specific reporting period is covered.

5. AUTHOR(S): Enter the name(s) of author(s) as shown on or in the report. Enter last name, first name, middle initial. If military, show rank and branch of service. The name of the principal author is an absolute minimum requirement.

6. REPORT DATE: Enter the date of the report as day, month, year; or month, year. If more than one date appears on the report, use date of publication.

7a. TOTAL NUMBER OF PAGES: The total page count should follow normal pagination procedures, i.e., enter the number of pages containing information.

7b. NUMBER OF REFERENCES: Enter the total number of references cited in the report.

8a. CONTRACT OR GRANT NUMBER: If appropriate, enter the applicable number of the contract or grant under which the report was written.

8b, 8c, & 8d. PROJECT NUMBER: Enter the appropriate military department identification, such as project number, subproject number, system numbers, task number, etc.

9a. ORIGINATOR'S REPORT NUMBER(S): Enter the official report number by which the document will be identified and controlled by the originating activity. This number must be unique to this report.

9b. OTHER REPORT NUMBER(S): If the report has been assigned any other report numbers (either by the originator or by the sponsor), also enter this number(s).

10. AVAILABILITY/LIMITATION NOTICES: Enter any limitations on further dissemination of the report, other than those imposed by security classification, using standard statements such as:

(1) "Qualified requesters may obtain copies of this report from DDC."

(2) "Foreign announcement and dissemination of this report by DDC is not authorized."

(3) "U. S. Government agencies may obtain copies of this report directly from DDC. Other qualified DDC users shall request through _____."

(4) "U. S. military agencies may obtain copies of this report directly from DDC. Other qualified users shall request through _____."

(5) "All distribution of this report is controlled. Qualified DDC users shall request through _____."

If the report has been furnished to the Office of Technical Services, Department of Commerce, for sale to the public, indicate this fact and enter the price, if known.

11. SUPPLEMENTARY NOTES: Use for additional explanatory notes.

12. SPONSORING MILITARY ACTIVITY: Enter the name of the departmental project office or laboratory sponsoring (paying for) the research and development. Include address.

13. ABSTRACT: Enter an abstract giving a brief and factual summary of the document indicative of the report, even though it may also appear elsewhere in the body of the technical report. If additional space is required, a continuation sheet shall be attached.

It is highly desirable that the abstract of classified reports be unclassified. Each paragraph of the abstract shall end with an indication of the military security classification of the information in the paragraph, represented as (TS), (S), (C), or (U).

There is no limitation on the length of the abstract. However, the suggested length is from 150 to 225 words.

14. KEY WORDS: Key words are technically meaningful terms or short phrases that characterize a report and may be used as index entries for cataloging the report. Key words must be selected so that no security classification is required. Identifiers, such as equipment model designation, trade name, military project code name, geographic location, may be used as key words but will be followed by an indication of technical context. The assignment of links, roles, and weights is optional.

DD FORM 1 JAN 64 1473

Security Classification

Distribution list as of March 1, 1965

1 Dr. Chalmers Sherwin
Deputy Director (Research & Technology)
DD&RE Rm 3E1060
The Pentagon
Washington, D. C. 20301

1 Dr. Edward M. Reilley
Asst. Director (Research)
Ofc. of Defense Res & Eng
Department of Defense
Washington, D. C. 20301

1 Dr. James A. Ward
Office of Deputy Director (Research and Information Rm 3D1037)
Department of Defense
The Pentagon
Washington, D. C. 20301

1 Director
Advanced Research Projects Agency
Department of Defense
Washington, D. C. 20301

1 Mr. Charles Yost, Director
for Materials Sciences
Advanced Research Projects Agency
Department of Defense
Washington, D. C. 20301

20 Defense Documentation Center
Cameron Station, Bldg. 5
Alexandria, Virginia 22314
Attn: TISIA

1 Director
National Security Agency
Fort George G. Meade, Maryland 20755
Attn: Librarian C-332

1 Chief of Research and Development
Headquarters, Department of the Army
Washington, D. C. 20310
Attn: Physical Sciences Division P & E

1 Chief of Research and Development
Headquarters, Department of the Army
Washington, D. C. 20310
Attn: Mr. L. H. Geiger, Rm 34442

1 Research Plans Office
U. S. Army Research Office
3045 Columbia Pike
Arlington, Virginia 22204

1 Commanding General
U. S. Army Materiel Command
Attn: AMCRD-RS-PE-E
Washington, D. C. 20315

1 Commanding General
U. S. Army Strategic Communications Command
Washington, D. C. 20315

1 Commanding Officer
U. S. Army Materials Research Agency
Watertown Arsenal
Watertown, Massachusetts 02172

1 Commanding Officer
U. S. Army Ballistics Research Lab.
Aberdeen Proving Ground
Aberdeen, Maryland 21005
Attn: V. W. Richards

1 Commanding Officer
U. S. Army Ballistics Research Lab.
Aberdeen Proving Ground
Aberdeen, Maryland 21005
Attn: Keats A. Pullen, Jr.

1 Commanding Officer
U. S. Army Ballistics Research Lab.
Aberdeen Proving Ground
Aberdeen, Maryland 21005
Attn: George C. Francis, Computing Lab.

1 Commandant
U. S. Army Air Defense School
P. O. Box 9390
Fort Bliss, Texas 79916
Attn: Missile Sciences Div., C&S Dept.

1 Commanding General
U. S. Army Missile Command
Redstone Arsenal, Alabama 35809
Attn: Technical Library

1 Commanding General
Frankford Arsenal
Philadelphia, Pa. 19137
Attn: SMUFA-1310 (Dr. Sidney Ross)

1 Commanding General
Frankford Arsenal
Philadelphia, Pa. 19137
Attn: SMUFA-1300

1 U. S. Army Munitions Command
Picatinney Arsenal
Dover, New Jersey 07801
Attn: Technical Information Branch

1 Commanding Officer
Harry Diamond Laboratories
Connecticut Ave. & Van Ness St., N.W.
Washington, D. C. 20438
Attn: Mr. Berthold Altman

1 Commanding Officer
Harry Diamond Laboratories
Attn: Library
Connecticut Ave. & Van Ness St., N.W.
Washington, D. C. 20438

1 Commanding Officer
U. S. Army Security Agency
Arlington Hall
Arlington, Virginia 22212

1 Commanding Officer
U. S. Army Limited War Laboratory
Aberdeen Proving Ground
Aberdeen, Maryland 21005
Attn: Technical Director

1 Commanding Officer
Human Engineering Laboratories
Aberdeen Proving Ground, Maryland 21005

1 Director
U. S. Army EngineerGeodesy, Intelligence and Mapping, Research & Devel. Agency
Fort Belvoir, Virginia 22060

1 Commandant
U. S. Army Command and General Staff College
Fort Leavenworth, Kansas 66207
Attn: Secretary

1 Dr. H. Robl, Deputy Director
U. S. Army Research Office (Durham)
Box CM, Duke Station
Durham, North Carolina 27706

1 Commanding Officer
U. S. Army Research Office (Durham)
P. O. Box CM, Duke Station
Durham, North Carolina 27706
Attn: CRD-AA-IP (Richard O. Ulsh)

1 Commanding General
U. S. Army Electronics Command
Fort Monmouth, New Jersey 07703
Attn: AMSEL-SC

1 Director
U. S. Army Electronics Laboratories
Fort Monmouth, New Jersey 07703
Attn: Dr. S. Benedict Levin, Director
Institute for Exploratory Research

1 Director
U. S. Army Electronics Laboratories
Fort Monmouth, New Jersey 07703
Attn: Mr. Robert O. Parker, Executive
Secretary, JSTAC (AMSEL-RD-X)

1 Superintendent
U. S. Military Academy
West Point, New York 10996

1 The Walter Reed Institute of Research
Walter Reed Army Medical Center
Washington, D. C. 20012

1 Director
U. S. Army Electronics Laboratories
Fort Monmouth, New Jersey 07703
Attn: AMSEL-RD-DR

1 Director
U. S. Army Electronics Laboratories
Attn: AMSEL-RD-X
Fort Monmouth, New Jersey 07703

1 Director
U. S. Army Electronics Laboratories
Fort Monmouth, New Jersey 07703
Attn: AMSEL-RD-XE

1 Director
U. S. Army Electronics Laboratories
Fort Monmouth, New Jersey 07703
Attn: AMSEL-RD-XC

1 Director
U. S. Army Electronics Laboratories
Fort Monmouth, New Jersey 07703
Attn: AMSEL-RD-XS

1 Director
U. S. Army Electronics Laboratories
Fort Monmouth, New Jersey 07703
Attn: AMSEL-RD-NR

1 Director
U. S. Army Electronics Laboratories
Fort Monmouth, New Jersey 07703
Attn: AMSEL-RD-NE

1 Director
U. S. Army Electronics Laboratories
Fort Monmouth, New Jersey 07703
Attn: AMSEL-RD-NO

1 Director
U. S. Army Electronics Laboratories
Fort Monmouth, New Jersey 07703
Attn: AMSEL-RD-NP

1 Director
U. S. Army Electronics Laboratories
Fort Monmouth, New Jersey 07703
Attn: AMSEL-RD-SA

1 Director
U. S. Army Electronics Laboratories
Fort Monmouth, New Jersey 07703
Attn: AMSEL-RD-SE

1 Director
U. S. Army Electronics Laboratories
Fort Monmouth, New Jersey 07703
Attn: AMSEL-RD-SR

1 Director
U. S. Army Electronics Laboratories
Fort Monmouth, New Jersey 07703
Attn: AMSEL-RD-SS

1 Director
U. S. Army Electronics Laboratories
Fort Monmouth, New Jersey 07703
Attn: AMSEL-RD-PE

1 Director
U. S. Army Electronics Laboratories
Fort Monmouth, New Jersey 07703
Attn: AMSEL-RD-PF

1 Director
U. S. Army Electronics Laboratories
Fort Monmouth, New Jersey 07703
Attn: AMSEL-RD-PR

1 Director
U. S. Army Electronics Laboratories
Fort Monmouth, New Jersey 07703
Attn: AMSEL-RL-GF

1 Director
U. S. Army Electronics Laboratories
Fort Monmouth, New Jersey 07703
Attn: AMSEL-RD-ADT

1 Director
U. S. Army Electronics Laboratories
Fort Monmouth, New Jersey 07703
Attn: AMSEL-RD-FU#1

1 Commanding Officer
U. S. Army Electronics R&D Activity
Fort Huachuca, Arizona 85163

1 Commanding Officer
U. S. Army Engineers R&D Laboratory
Fort Belvoir, Virginia 22060
Attn: STINFO Branch

1 Commanding Officer
U. S. Army Electronics R&D Activity
White Sands Missile Range
New Mexico 88002

1 Director
Human Resources Research Office
The George Washington University
300 N. Washington Street
Alexandria, Virginia

1 Commanding Officer
U. S. Army Personnel Research Office
Washington 25, D. C.

1 Commanding Officer
U. S. Army Medical Research Laboratory
Fort Knox, Kentucky

1 Commanding General
U. S. Army Signal Center and School
Attn: Chief, Office of Academic Operations
Fort Monmouth, New Jersey 07703

2 Dr. Richard H. Wilcox, Code 437
Department of the Navy
Washington, D. C. 20360

1 Chief, Bureau of Weapons
Attn: Technical Library, DL1-3
Department of the Navy
Washington, D. C. 20360

1 Chief, Bureau of Ships
Department of the Navy
Washington, D. C. 20360
Attn: Code 680

1 Chief, Bureau of Ships
Department of the Navy
Washington, D. C. 20360
Attn: Code 732

1 Commander
U. S. Naval Air Development Center
Johnsville, Pennsylvania
Attn: NADC Library

1 Commanding Officer
Naval Electronics Laboratory
San Diego, California 92052
Attn: Code 2222(Library)

1 Commanding Officer
Naval Electronics Laboratory
San Diego, California 92052
Attn: Code 2800, C. S. Manning

1 Commanding Officer and Director
(Code 142 Library)
David W. Taylor Model Basin
Washington, D. C. 20007

6 Director
Naval Research Laboratory
Washington, D. C. 20390
Attn: Technical Information Office (Code 2000)

1 Commanding Officer
Office of Naval Research Branch Office
219 S. Dearborn Street
Chicago, Illinois 60604

1 Chief of Naval Operations
Department of the Navy
Washington, D. C. 20350
Attn: OP-07T

1 Chief of Naval Operations
Department of the Navy
Washington, D. C. 20350
Attn: OP-03EG

1 Commanding Officer
Office of Naval Research Branch Office
1000 Geary Street
San Francisco, California 94109

1 Commanding Officer
U. S. Naval Weapons Laboratory
Asst. Director for Computation
Dahlgren, Virginia 22448
Attn: G. H. Gleissner (Code K-4)

1 Inspector of Naval Material
Bureau of Ships Technical Representative
1902 West Minnehaha Avenue
St. Paul 4, Minnesota

5 Lt. Col. E. T. Gaines, SREE
Chief, Electronics Division
Directorate of Engineering Sciences
Air Force Office of Scientific Research
Washington, D. C. 20333

1 Director of Science & Technology
Deputy Chief of Staff (R & D)
USAF
Washington, D. C.
Attn: AFRST-EL/GU

1 Director of Science & Technology
Deputy Chief of Staff (R & D)
USAF
Washington, D. C.
Attn: AFRST-SC

1 Karl M. Fuechsel
Electronics Division
Director of Engineering Sciences
Air Force Office of Scientific Research
Washington, D. C. 20333

1 Lt. Col. Edwin M. Myers
Headquarters, USAF (AFRDR)
Washington 25, D. C.

1 Director, Air University Library
Maxwell Air Force Base
Alabama 36112
Attn: CR-4803a

1 Commander
Research & Technology Division
AFSC (Mr. Robert L. Feik)
Office of the Scientific Director
Bolling AFB 25, D. C.

1 Commander
Research & Technology Division
Office of the Scientific Director
Bolling AFB 25, D. C.
Attn: RTHR

1 Commander
Air Force Cambridge Research Laboratories
Attn: Research Library
CRMXL-R
L. G. Hanscom Field
Bedford, Massachusetts 01731

1 Dr. Lloyd Hollingsworth
AFCRL
L. G. Hanscom Field
Bedford, Massachusetts 01731

1 Commander
Air Force Cambridge Research Laboratories
Attn: Data Sciences Lab
(Lt. S. J. Kahne, CRB)
L. G. Hanscom Field
Bedford, Massachusetts 01731

1 Commander
Air Force Systems Command
Office of the Chief Scientist
(Mr. A. G. Wimer)
Andrews AFB, Maryland 20331

1 Commander
Air Force Missile Development Center
Attn: MDSGO/Major Harold Wheeler, Jr.
Holloman Air Force Base, New Mexico

1 Commander
Research & Technology Division
Attn: MAYT (Mr. Evans)
Wright-Patterson Air Force Base
Ohio 45433

1 Directorate of Systems Dynamics Analysis
Aeronautical Systems Division
Wright-Patterson AFB, Ohio 45433

1 Hqs. Aeronautical Systems Division
AF Systems Command
Attn: Navigation & Guidance Laboratory
Wright-Patterson AFB, Ohio 45433

1 Commander
Rome Air Development Center
Attn: Documents Library, RAALD
Griffiss Air Force Base
Rome, New York 13442

1 Commander
Rome Air Development Center
Attn: RAWI-Major W. H. Harris
Griffiss Air Force Base
Rome, New York 13442

1 Lincoln Laboratory
Massachusetts Institute of Technology
P. O. Box 73
Lexington 73, Massachusetts
Attn: Library A-082

Continued next page

Distribution list as of March 1, 1965 (Cont'd.)

1 Lincoln Laboratory
Massachusetts Institute of Technology
P. O. Box 73
Lexington 73, Massachusetts
Attn: Dr. Robert Kingston

1 APGC (PGAPI)
Eglin Air Force Base
Florida

1 Mr. Alan Barnum
Rome Air Development Center
Griffiss Air Force Base
Rome, New York 13442

1 Director
Research Laboratory of Electronics
Massachusetts Institute of Technology
Cambridge, Massachusetts 02139

1 Polytechnic Institute of Brooklyn
55 Johnson Street
Brooklyn, New York 11201
Attn: Mr. Jerome Fox
Research Coordinator

1 Director
Columbia Radiation Laboratory
Columbia University
538 West 120th Street
New York, New York 10027

1 Director
Coordinated Science Laboratory
University of Illinois
Urbana, Illinois 61803

1 Director
Stanford Electronics Laboratories
Stanford University
Stanford, California

1 Director
Electronics Research Laboratory
University of California
Berkeley 4, California

1 Professor A. A. Dougal, Director
Laboratories for Electronics and Related
Science Research
University of Texas
Austin, Texas 78712

1 Professor J. K. Aggarwal
Department of Electrical Engineering
University of Texas
Austin, Texas 78712

1 Director of Engineering & Applied Physics
210 Pierce Hall
Harvard University
Cambridge, Massachusetts 02138

1 Capt. Paul Johnson (USN Ret.)
National Aeronautics & Space Agency
1520 H. Street, N. W.
Washington 25, D. C.

1 NASA Headquarters
Office of Applications
400 Maryland Avenue, S.Q.
Washington 25, D. C.
Attn: Code FC Mr. A. M. Greg Andrus

1 National Bureau of Standards
Research Information Center and Advisory
Serv. on Info. Processing
Data Processing Systems Division
Washington 25, D. C.

1 Dr. Wallace Sinaiko
Institute for Defense Analyses
Research & Eng. Support Div.
1666 Connecticut Avenue, N. W.
Washington 9, D. C.

1 Data Processing Systems Division
National Bureau of Standards
Conn. at Van Ness
Room 239, Bldg. 10
Washington 25, D. C.
Attn: A. K. Smilow

1 Exchange and Gift Division
The Library of Congress
Washington 25, D. C.

1 Dr. Alan T. Waterman, Director
National Science Foundation
Washington 25, D. C.

1 H. E. Cochran
Oak Ridge National Laboratory
P. O. Box X
Oak Ridge, Tennessee

1 U. S. Atomic Energy Commission
Office of Technical Information Extension
P. O. Box 62
Oak Ridge, Tennessee

1 Mr. G. D. Watson
Defense Research Member
Canadian Joint Staff
2450 Massachusetts Avenue, N. W.
Washington 8, D. C.

1 Martin Company
P. O. Box 5837
Orlando, Florida
Attn: Engineering Library MP-30

1 Laboratories for Applied Sciences
University of Chicago
6220 South Drexel
Chicago, Illinois 60637

1 Librarian
School of Electrical Engineering
Purdue University
Lafayette, Indiana

1 Donald L. Epley
Dept. of Electrical Engineering
State University of Iowa
Iowa City, Iowa

1 Instrumentation Laboratory
Massachusetts Institute of Technology
68 Albany Street
Cambridge 39, Massachusetts
Attn: Library WI-109

1 Sylvania Electric Products, Inc.
Electronics System
Waltham Labs. Library
100 First Avenue
Waltham 54, Massachusetts

2 Hughes Aircraft Company
Centinela and Teale Streets
Culver City, California
Attn: K. C. Rosenberg, Supervisor
Company Technical Document Center

3 Autonetics
9150 East Imperial Highway
Downey, California
Attn: Tech. Library, 3041-11

1 Dr. Arnold T. Nordsieck
General Motors Corporation
Defense Research Laboratories
6767 Hollister Avenue
Goleta, California

1 University of California
Lawrence Radiation Laboratory
P. O. Box 808
Livermore, California

1 Mr. Thomas L. Hartwick
Aerospace Corporation
P. O. Box 95085
Los Angeles 45, California

1 Lt. Col. Willard Levin
Aerospace Corporation
P. O. Box 95085
Los Angeles 45, California

1 Sylvania Electronic Systems-West
Electronic Defense Laboratories
P. O. Box 205
Mountain View, California
Attn: Documents Center

1 Varian Associates
611 Hansen Way
Palo Alto, California 94303
Attn: Tech. Library

1 Huston Denslow
Library Supervisor
Jet Propulsion Laboratory
California Institute of Technology
Pasadena, California

1 Professor Nicholas George
California Institute of Technology
Electrical Engineering Department
Pasadena, California

1 Space Technology Labs., Inc.
One Space Park
Redondo Beach, California
Attn: Acquisitions Group
STL Technical Library

1 The Rand Corporation
1700 Main Street
Santa Monica, California
Attn: Library

1 Miss F. Cloak
Radio Corp. of America
RCA Laboratories
David Sarnoff Research Center
Princeton, New Jersey

1 Mr. A. A. Lundstrom
Bell Telephone Laboratories
Room 2E-127
Whippany Road
Whippany, New Jersey

1 Cornell Aeronautical Laboratory, Inc.
4455 Genesee Street
Buffalo 21, New York
Attn: J. P. Desmond, Librarian

1 Sperry Gyroscope Company
Marine Division Library
155 Glenn Cove Road
Carle Place, L. I., New York
Attn: Miss Barbara Judd

1 Library
Light Military Electronics Dept.
General Electric Company
Armament & Control Products Section
Johnson City, New York

1 Dr. E. Howard Holt
Director
Plasma Research Laboratory
Rennselaer Polytechnic Institute
Troy, New York

1 Battele-DEFENDER
Battelle Memorial Institute
505 King Avenue
Columbus 1, Ohio

1 Laboratory for Electroscience Research
New York University
University Heights
Bronx 53, New York

1 National Physical Laboratory
Teddington, Middlesex
England
Attn: Dr. A. M. Uttley, Superintendent,
Autonomics Division

1 Dr. Lee Huff
Behavioral Sciences
Advanced Research Projects Agency
The Pentagon (Room 3E175)
Washington, D. C. 20301

1 Dr. Glenn L. Bryan
Head, Personnel and Training Branch
Office of Naval Research
Navy Department
Washington, D. C. 20360

1 Instituto de Fisica Aplicado
"L. Torres Quevedo"
High Vacuum Laboratory
Madrid, Spain
Attn: Jose L. de Segovia

1 Stanford Research Institute
Attn: G-037 External Reports
(for J. Goldberg)
Menlo Park, California 94025

REVISED U. S. ARMY DISTRIBUTION LIST

(As received at the Coordinated Science Laboratory 27 July 1965)

1 Dr. Chalmers Sherwin
Deputy Director (Research & Technology)
DD&RE Rm 3E1060
The Pentagon
Washington, D. C. 20301

1 Dr. Edward M. Reilley
Asst. Director (Research)
Ofc. of Defense Res. & Eng.
Department of Defense
Washington, D. C. 20301

1 Dr. James A. Ward
Office of Deputy Director (Research and Information Rm 3D1037)
Department of Defense
The Pentagon
Washington, D. C. 20301

1 Director
Advanced Research Projects Agency
Department of Defense
Washington, D. C. 20301

1 Mr. E. I. Salkovitz, Director for Materials Sciences
Advanced Research Projects Agency
Department of Defense
Washington, D. C. 20301

1 Colonel Charles C. Mack
Headquarters
Defense Communications Agency (333)
The Pentagon
Washington, D. C. 20305

20 Defense Documentation Center
Attn: TISIA
Cameron Station, Building 5
Alexandria, Virginia 22314

1 Director
National Security Agency
Attn: Librarian C-332
Fort George G. Meade, Maryland 20755

1 U. S. Army Research Office
Attn: Physical Sciences Division
3045 Columbia Pike
Arlington, Virginia 22204

1 Chief of Research and Development
Headquarters, Department of the Army
Attn: Mr. L. H. Geiger, Rm 3D442
Washington, D. C. 20310

1 Research Plans Office
U. S. Army Research Office
3045 Columbia Pike
Arlington, Virginia 22204

1 Commanding General
U. S. Army Materiel Command
Attn: AMCRD-RS-PE-E
Washington, D. C. 20315

1 Commanding General
U. S. Army Strategic Communications Command
Washington, D. C. 20315

1 Commanding Officer
U. S. Army Materials Research Agency
Watertown Arsenal
Watertown, Massachusetts 02172

1 Commanding Officer
U. S. Army Ballistics Research Laboratory
Attn: V. W. Richards
Aberdeen Proving Ground
Aberdeen, Maryland 21005

1 Commanding Officer
U. S. Army Ballistics Research Laboratory
Attn: Keats A. Pullen, Jr.
Aberdeen Proving Ground
Aberdeen, Maryland 21005

1 Commanding Officer
U. S. Army Ballistics Research Laboratory
Attn: George C. Francis, Computing Lab.
Aberdeen Proving Ground, Maryland 21005

1 Commandant
U. S. Army Air Defense School
Attn: Missile Sciences Division, C&S Dept.
P. O. Box 9390
Fort Bliss, Texas 79916

1 Commanding General
U. S. Army Missile Command
Attn: Technical Library
Redstone Arsenal, Alabama 35809

1 Commanding General
Frankford Arsenal
Attn: SMUFA-1310 (Dr. Sidney Ross)
Philadelphia, Pennsylvania 19137

1 Commanding General
Frankford Arsenal
Attn: SMUFA-1300
Philadelphia, Pennsylvania 19137

1 U. S. Army Munitions Command
Attn: Technical Information Branch
Picatinney Arsenal
Dover, New Jersey 07801

1 Commanding Officer
Harry Diamond Laboratories
Attn: Mr. Berthold Altman
Connecticut Avenue and Van Ness St.,N.W.
Washington, D. C. 20438

1 Commanding Officer
Harry Diamond Laboratories
Attn: Library
Connecticut Avenue and Van Ness St.,N.W.
Washington, D. C. 20438

1 Commanding Officer
U. S. Army Security Agency
Arlington Hall
Arlington, Virginia 22212

1 Commanding Officer
U. S. Army Limited War Laboratory
Attn: Technical Director
Aberdeen Proving Ground
Aberdeen, Maryland 21005

1 Commanding Officer
Human Engineering Laboratories
Aberdeen Proving Ground, Maryland 21005

1 Director
U. S. Army Engineer Geodesy, Intelligence & Mapping
Research and Development Agency
Fort Belvoir, Virginia 22060

1 Commandant
U. S. Army Command and General Staff College
Attn: Secretary
Fort Leavenworth, Kansas 66207

1 Dr. H. Robl, Deputy Chief Scientist
U. S. Army Research Office (Durham)
Box CM, Duke Station
Durham, North Carolina 27706

1 Commanding Officer
U. S. Army Research Office (Durham)
Attn: CRD-AA-IP (Richard O. Ulsh)
Box CM, Duke Station
Durham, North Carolina 27706

1 Superintendent
U. S. Army Military Academy
West Point, New York 10996

1 The Walter Reed Institute of Research
Walter Reed Army Medical Center
Washington, D. C. 20012

1 Commanding Officer
U. S. Army Electronics R&D Activity
Fort Huachuca, Arizona 85163

1 Commanding Officer
U. S. Army Engineers R&D Laboratory
Attn: STINFO Branch
Fort Belvoir, Virginia 22060

1 Commanding Officer
U. S. Army Electronics R&D Activity
White Sands Missile Range, New Mexico 88002

1 Director
Human Resources Research Office
The George Washington University
300 N. Washington Street
Alexandria, Virginia 22300

1 Commanding Officer
U. S. Army Personnel Research Office
Washington, D. C.

1 Commanding Officer
U. S. Army Medical Research Laboratory
Fort Knox, Kentucky 40120

1 Commanding General
U. S. Army Signal Center and School
Fort Monmouth, New Jersey 07703
Attn: Chief, Office of Academic Operations

1 Dr. S. Benedict Levin, Director
Institute for Exploratory Research
U. S. Army Electronics Command
Fort Monmouth, New Jersey 07703

1 Director
Institute for Exploratory Research
U. S. Army Electronics Command
Attn: Mr. Robert O. Parker, Executive Secretary, JSTAC (AMSEL-XL-D)
Fort Monmouth, New Jersey 07703

1 Commanding General
U. S. Army Electronics Command
Fort Monmouth, New Jersey 07703

Attn: AMSEL-SC
RD-D
RD-G
RD-MAF-I
RD-MAT
RD-GF
RD-MN (Marine Corps LnO)
XL-D
XL-E
XL-C
XL-S
HL-D
HL-L
HL-J
HL-P
HL-O
HL-R
NL-D
NL-A
NL-P
NL-R
NL-S
KL-D
KL-E
KL-S
KL-T
VL-D
WL-D

1 Mr. Charles F. Yost
Special Assistant to the Director of Research
National Aeronautics & Space Admin.
Washington, D. C. 20546

1 Director
Research Laboratory of Electronics
Massachusetts Institute of Technology
Cambridge, Massachusetts 02139

1 Polytechnic Institute of Brooklyn
55 Johnson Street
Brooklyn, New York 11201
Attn: Mr. Jerome Fox
Research Coordinator

1 Director
Columbia Radiation Laboratory
Columbia University
538 West 120th Street
New York, New York 10027

1 Director
Stanford Electronics Laboratories
Stanford University
Stanford, California 94301

1 Director
Electronics Research Laboratory
University of California
Berkeley, California 94700

1 Director
Electronic Sciences Laboratory
University of Southern California
Los Angeles, California 90007

1 Professor A. A. Dougal, Director
Laboratories for Electronics and Related Science Research
University of Texas
Austin, Texas 78712

1 Professor J. K. Aggarwal
Department of Electrical Engineering
University of Texas
Austin, Texas 78712

1 Division of Engineering and Applied Physics
210 Pierce Hall
Harvard University
Cambridge, Massachusetts 02138